3

Analysis of the Lead Sensitivity Distribution in Implantable Cardioverter Defibrillator

Jesús Requena-Carrión[1], Juho Väisänen[2],
Jari Hyttinen[2] and Juan J. Vinagre-Díaz[1]
[1]*University Rey Juan Carlos*
[2]*Tampere University of Technology*
[1]*Spain*
[2]*Finland*

1. Introduction

Most current Implantable Cardioverter Defibrillators (ICD) use intracardiac leads for electrogram (EGM) sensing and defibrillation (Belott & Reynolds, 2007). Intracardiac leads consist of several electrodes that for the basic functionality of ventricular tachyarrhythmia detection and termination, are inserted transvenously into the right ventricle (Gradaus et al., 2003; Swerdlow et al., 2007). In addition to intracardiac electrodes, ICD also use the casing of the implant as an indifferent, distant electrode.

In ICD technology, three main intracardiac lead configurations are distinguished based on the combination of electrodes that they use, namely unipolar, dedicated bipolar and integrated bipolar. Unipolar leads, so-called because they use the casing of the implant as an indifferent electrode, consist of a single electrode located in the right ventricle, whereas bipolar leads, both dedicated and integrated, consist of two closely spaced electrodes located in the right ventricle. In general, unipolar lead configurations are used for cardiac defibrillation, while bipolar lead configurations are used for EGM sensing, i.e. they provide with the EGM signals from which heart rhythm can be extracted.

Previous studies indicate that lead configuration can affect EGM sensing and ICD performance. For instance, it is well known that fundamental EGM features such as wave duration, wave amplitude and power spectrum, depend on the configuration of the recording leads (DeCaprio et al., 1977; Jenkins, 1992; Langberg et al., 1988; Parsonnet et al., 1980). Also, differences in ventricular fibrillation detection and redetection times have been reported when comparing ICD dedicated and integrated bipolar leads (Cooklin et al., 1999; Frain et al., 2007; Goldberger et al., 1998; Natale et al., 1996). Other studies have addressed the effects on EGM sensing, of artifacts originating from non-ventricular bioelectric sources. For example, inappropriate ICD discharges have been ascribed to myopotentials oversensing (Deshmukh & Anderson, 1998; Kowalski et al., 2008; Sandler & Kutalek, 1994; Schulte et al., 2001). Pacing stimulus artifacts, which are often associated to ICD undersensing, have been found to be greater in integrated than in dedicated bipolar leads (Menz et al., 1998). Finally, an optimized lead design for atrial sensing has been proposed, in order to facilitate rejection of artifacts such as R-waves and myopotentials (Nash et al., 2005). Therefore, the existing

evidence indicates that by carefully designing ICD intracardiac leads, EGM sensing and hence ICD overall performance can be further improved.

The effects of lead configuration on ICD sensing performance can be explored through the notion of lead sensitivity distribution, also known as lead field. The lead sensitivity distribution describes the ability of leads to measure the electrical activity generated by bioelectric organs and tissues in the body and hence, it can help to identify the sources of bioelectric artifacts and to quantify their effects. In addition to this, the analysis of the lead sensitivity distribution can contribute to widen the range of functionality of ICD systems by providing with an estimation of lead spatial resolution. The quantification of the lead spatial resolution could be of great interest, especially in those scenarios where the underlying cardiac pathology is caused by local physiological abnormalities such as myocardial ischemia (Asbach et al., 2006; Bunch & Day, 2008; Williams et al., 2008), or when the underlying pathology can be related to tissue spatial heterogeneities (Zaitsev et al., 2000).

The sensitivity distributions of two unipolar and two bipolar ICD intracardiac lead configurations have been investigated in a previous study (Requena-Carrión et al., 2009). By combining a detailed numerical model of the human thorax and finite difference methods (FDM), the sensitivity distribution at the ventricles of each lead configuration was obtained. The sensitivity distribution also allowed to quantify the spatial resolution of each lead configuration, and significant differences in sensing between different lead configurations were found. However, a more complete picture of EGM sensing in ICD should account for the measurement of the activity of other bioelectric sources that could affect ICD performance, such as myopotentials. The analysis of the sensitivity of intracardiac leads at other bioelectric sources in the human body would improve our understanding on how electrophysiological artifacts affect EGM sensing and therefore, it would help to devise new strategies to reject such artifacts by means of designing new lead configurations.

In this study, the sensitivity distribution of four ICD intracardiac lead configurations is calculated at the ventricles, the atria and near skeletal muscles. For that purpose, a detailed computational model of the human thorax is used in combination with numerical methods. Additionally, a discrimination index which is based on the sensitivity distribution is used for quantifying differences in sensing at the ventricles, atria and near muscles. This discrimination index takes the accumulated sensitivity of ICD leads at the ventricles, where the signals of interest are originated, and compares it with the accumulated sensitivity at the other bioelectric sources.

2. Principles of bioelectric signals measurement

Bioelectric measurement models consist of two basic elements, namely a bioelectric source and a volume conductor (Malmivuo & Plonsey, 1995). The bioelectric source is the biological tissue or organ that generates electric currents for regulating a physiological function, whereas the volume conductor is the conducting medium in which the bioelectric source resides. Well-known examples of bioelectric sources are the heart, the brain and the skeletal muscle; the human body as a whole, on the other hand, behaves electrically as a volume conductor.

As a consequence of the activity of bioelectric sources, a time-varying voltage gradient is induced across the volume conductor. This voltage gradient can be measured by means of measurement leads, which consist of at least one pair of electrodes in contact with the volume conductor. From the point of view of the measurement leads, the time-varying measured voltage $u(t)$ can be modeled mathematically as a weighted linear combination of the currents

$\mathbf{J}(t,v)$ generated by the bioelectric source V:

$$u(t) = \int_V \mathbf{L}(v) \cdot \mathbf{J}(t,v) dv. \tag{1}$$

In this equation $\mathbf{L}(v)$ denotes the lead sensitivity distribution and it describes the ability of the lead to measure the bioelectric currents $\mathbf{J}(t,v)$ generated by the source at $v \in V$. In general, since the lead sensitivity distribution will be larger in some regions of the bioelectric source than in others, the contribution to the total measured voltage will vary from one region within the bioelectric source to another. As a consequence, it can be said that the lead sensitivity distribution focus the measurement on selected regions within the bioelectric source and therefore, the lead sensitivity distribution will define a characteristic lead spatial resolution.
Whenever more than one bioelectric source reside within the volume conductor, by virtue of the superposition principle the total voltage measured by the leads can be expressed as the sum of the voltages induced by each source independently. For example, if two sources V_1 and V_2 exist, the total voltage $u(t)$ will be expressed as:

$$u(t) = u_1(t) + u_2(t) = \int_{V_1} \mathbf{L}(v) \cdot \mathbf{J}(t,v) dv + \int_{V_2} \mathbf{L}(v) \cdot \mathbf{J}(t,v) dv, \tag{2}$$

where $u_1(t)$ and $u_2(t)$ are the voltages generated by sources V_1 and V_2, respectively. In this scenario, the lead sensitivity distribution will determine the contribution of each region V_1 and V_2 to the total measured voltage. If, for instance, $\mathbf{L}(v)$ is much larger in V_1 than in V_2, the contribution of V_1 to the total measured voltage $u(t)$ will be expected to be higher than the contribution of V_2. Consequently, the lead sensitivity distribution, in addition to define the lead spatial resolution, will also allow to investigate the ability of a measurement lead to discriminate between different bioelectric sources.
Since the lead sensitivity distribution depends on both the volume conductor and the design and arrangement of the measurement leads, different leads will be characterized by different measurement properties. Based on the analysis of the lead sensitivity distribution, several techniques have been devised in the literature for investigating how current lead systems measure bioelectric phenomena. One of the earliest and most popular methods is the analysis of iso-sensitivity surfaces, which consists of depicting the surfaces in the bioelectric source where the magnitude of the lead sensitivity distribution remains constant. This analysis method was used by Rush and Driscoll for describing electroencephalographic (EEG) leads (Rush & Driscoll, 1969) and by Arzbaecher et al. for investigating the sensitivity of precordial and esophageal electrocardiographic (ECG) leads (Arzbaecher et al., 1979).
The sensitivity distribution has also been the basis for quantifying the lead spatial resolution. Based on the estimation of iso-sensitivity surfaces, Malmivuo et al. proposed the half sensitivity volume (HSV), which was defined as the bioelectric region enclosed by the surface where the sensitivity magnitude drops to half of the maximum sensitivity (Malmivuo et al., 1997). By using the HSV, the spatial resolutions of EEG and magnetoencephalography systems were compared. Also, by combining sensitivity distribution models and numerical simulations of cardiac dynamics, Requena-Carrión et al. proposed the resolution volume (ResV) for quantifying lead spatial resolution (Requena-Carrión et al., 2007). The ResV was defined as the bioelectric region that contributes to a given fraction of the measured signal power, and it was used for quantifying the spatial resolution of surface ECG leads (Requena-Carrión et al., 2007) and intracardiac leads in ICD (Requena-Carrión et al., 2009). Finally, Väisänen et al. further explored the notion of lead spatial resolution by proposing

ICD Casing	Height (mm) Width (mm) Depth (mm)	64 51 15
Helix	Length (mm) Diameter (mm)	2 3
Ring	Length (mm) Diameter (mm)	3 3
Right ventricular coil	Length (mm) Diameter (mm)	57 3
Interelectrode spacing	Helix-Ring (mm) Helix-Coil (mm)	8 12

Table 1. Electrode specifications.

the region of interest sensitivity ratio (ROISR), defined as the ratio between the average sensitivities of any two regions within the bioelectric source (Väisänen et al., 2008). The ROISR allowed to quantify the specificity of EEG (Väisänen et al., 2008) and surface ECG measurements (Väisänen & Hyttinen, 2009).
In summary, the lead sensitivity distribution constitutes both a useful theoretical tool for understanding the nature of bioelectric signals, and a useful practical tool for describing quantitatively the sensing properties of measurement leads. In this study, the sensitivity distribution will be used to quantify and compare the ability of four ICD intracardiac leads to measure ventricular bioelectrical events and reject bioelectrical artifacts from the atria and near muscles. For that purpose, the sensitivity distribution of each lead configuration under investigation will be analyzed and in addition to this, a measure of discrimination based on the sensitivity distribution will be proposed.

3. Methods

3.1 Intracardiac ICD leads

The measurement properties of four ICD intracardiac lead configurations (two unipolar, one dedicated bipolar and one integrated bipolar) were investigated. In order to define the geometry and the anatomical location of the electrodes that formed each intracardiac lead, a commercial ICD system was used as a reference model. This system consisted of two elements, namely the Medtronic Secura ICD (Medtronic, 2008) and the Medtronic Sprint Quattro Secure ventricular lead (Medtronic, 2010). The Medtronic Secura ICD is a single chamber ICD which is used in combination with a right ventricular lead for analyzing heart rhythm and providing defibrillation, cardioversion and both bradycardia and antitachycardia pacing therapies. As for the Medtronic Sprint Quattro Secure, it is a quadripolar ventricular lead designed for pacing, sensing, cardioversion and defibrillation therapies.
The Secura ICD is intended to be located in the pectoral region. Its casing, which can be used as an indifferent, distant electrode, has the physical dimensions shown in Table 1. As for the Sprint Quattro Secure ventricular lead, it consists of a helix electrode located at the tip of the lead, followed consecutively by a ring electrode, a right ventricular coil and a superior vena cava coil. The helix and the ring electrode are used for EGM sensing and pacing, while both coils in combination with the ICD casing are used for defibrillation. Since this study focuses

Unipolar *A*	helix to casing
Unipolar *B*	coil to casing
Dedicated bipolar	helix to ring
Integrated bipolar	helix to coil

Table 2. Intracardiac leads definition.

on bioelectric measurement of ventricular events, the electrodes that were considered were the helix, the ring and the right ventricular coil. The physical dimensions and relative distances of the electrodes that were considered for this study are shown in Table 1.
Based on the aforementioned electrode specifications, the four intracardiac ICD leads were defined as follows (Table 2): the unipolar *A* lead used the casing of the implant and the helix electrode; the unipolar *B* lead used the casing of the implant and the right ventricular coil; the dedicated bipolar lead used the helix and the ring electrodes and finally, the integrated bipolar lead used the helix electrode and the right ventricular coil.

3.2 Computational model of the human thorax

A realistic 3D computational model of the bioelectric properties of the human thorax was implemented for calculating the lead sensitivity distributions. This computational model was defined based on the widely used Visible Human Man dataset, and consisted of a 341×594×394 cubic grid with a 1 mm×1 mm×1 mm resolution (Sachse et al., 1998). The human thorax model was segmented into 20 different organ and tissue types, including the atria, the ventricles and near muscles, and they were assigned resistivity values previously reported in the literature (Gabriel et al., 1996).
Lead sensitivity distributions were calculated in the realistic human thorax by applying the principle of reciprocity (Malmivuo & Plonsey, 1995), which states that when a lead is reciprocally energized, the current field that is induced in the volume conductor corresponds to the lead sensitivity distribution. An FDM approach was developed for calculating the current field induced in the realistic human thorax when each electrode pair was reciprocally energized. The FDM solver was based on the Incomplete Cholesky Preconditioner and Conjugate Gradient (Takano, 2002) and was executed on an AMD 3000+ 64Bit, 2 GB RAM, 200GB SATA RAID computer.

3.3 Discrimination power

Lead sensitivities at the ventricles were compared to lead sensitivities at the atria and near muscles. For that purpose, two discrimination indices based on the notion of ROISR (Väisänen et al., 2008) were defined as follows:

$$di_{AV} = \frac{\int_{atria} |\mathbf{L}(v)| dv}{\int_{ventricles} |\mathbf{L}(v)| dv} \qquad (3)$$

$$di_{MV} = \frac{\int_{muscle} |\mathbf{L}(v)| dv}{\int_{ventricles} |\mathbf{L}(v)| dv}$$

The discrimination index di_{AV} allowed to compare the accumulated sensitivities at the atria with the accumulated sensitivities at the ventricles, whereas the di_{MV} allowed to compare the

accumulated sensitivities at near skeletal muscles with the accumulated sensitivities at the ventricles. A logarithmic transformation was subsequently applied to both indices:

$$DI_{AV} = 20\log_{10}(di_{AV}) \qquad (4)$$
$$DI_{MV} = 20\log_{10}(di_{MV})$$

Consequently, the lower the value of a discrimination index for a given lead, the lower the sensitivity of that lead to the corresponding non-ventricular source (atria or skeletal muscle) and therefore, the lower the effects of bioelectric artifacts from that source.

4. Results

The analysis of the sensitivity distribution of each intracardiac lead reveals that, irrespective of the lead configuration and design, sensitivity is always higher at the close proximity of the electrodes and decreases with the distance. Specifically, as shown in Figures 1 and 2, the sensitivity of configurations using the signal provided by the helix electrode, i.e. unipolar A, dedicated bipolar and integrated bipolar, is highest near the ventricular apex, into which the helix electrode is usually inserted; similarly, the sensitivity across the ventricular septum is significantly higher in configurations using the right ventricular coil, i.e. unipolar B and integrated bipolar configurations. Figures 1 and 2 also show that the sensitivity of unipolar configurations decreases more slowly with the distance to the electrodes than the sensitivity of bipolar configurations and therefore, unipolar measurements are more uniform throughout the heart than bipolar measurements. In other words, bipolar configurations concentrate their measurements more than unipolar configurations.

As a consequence of the previous observation, since intracardiac ICD leads are inserted into the right ventricle, their sensitivity at the ventricular myocardium is higher than at the atrial myocardium. However, it is worth noting that the sensitivity distribution at the atria depends on the configuration of the lead. As seen in Figures 1 and 2, in the case of unipolar configurations the sensitivity distribution at the atria is of roughly the same order of magnitude as the sensitivity distribution at the ventricles, whereas in the case of bipolar configurations, the sensitivity distribution drops several orders of magnitude. In addition to this, by comparing bipolar configurations it can be concluded that the sensitivity at the atria is higher in the case of integrated bipolar than in the case of dedicated bipolar. Finally, by invoking the same physical principle according to which lead sensitivity decreases with the distance to the electrodes, since ICD are usually implanted in the pectoral area, the sensitivity at the pectoral muscle will be higher for unipolar leads, in which the casing of the implant acts as the indifferent electrode.

By calculating the discrimination indices DI_{AV} and DI_{MV}, the previous qualitative observations based on the analysis of the sensitivity distribution can be quantitatively contrasted. As Table 3 shows, the accumulated sensitivity of bipolar leads is several orders of magnitude higher at the ventricles than at the other non-ventricular bioelectric sources, namely the atria and near muscles. In addition to this, it can be noticed that dedicated bipolar configurations have a higher discrimination power than integrated bipolar configurations. Unipolar configurations, on the contrary, are characterized by a lower discrimination power, especially against muscular artifacts due to the proximity to the casing of the ICD. In general, it can be concluded from this analysis that the unipolar B configuration using the right ventricular coil and the casing of the implant, is the most vulnerable intracardiac configuration, whereas the dedicated bipolar configuration is the most robust configuration against bioelectric artifacts.

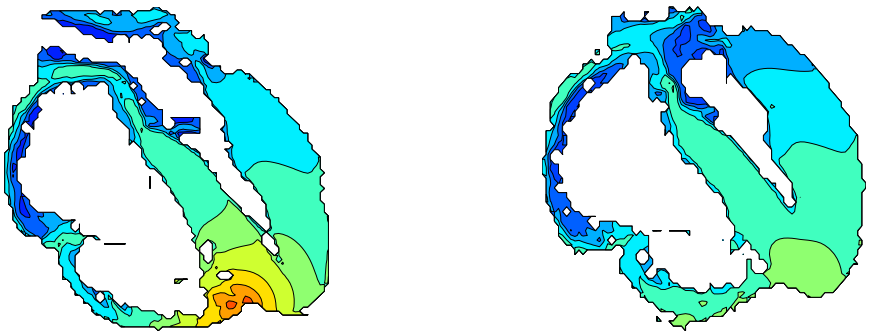

Unipolar *A* configuration (helix to casing)

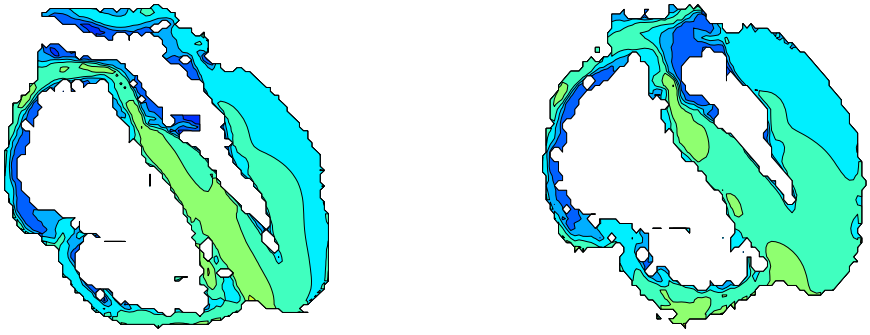

Unipolar *B* configuration (coil to casing)

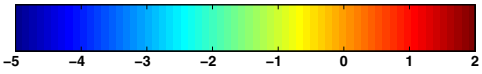

Fig. 1. Sensitivity distributions of unipolar intracardiac configurations at two cross-sections of the heart (arbitrary units, logarithmic scale).

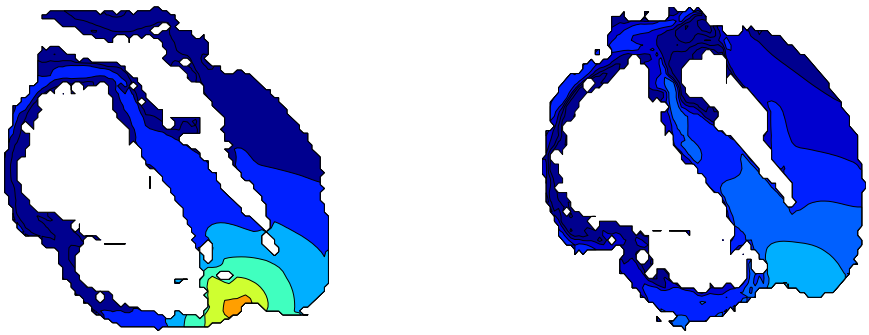

Dedicated bipolar configuration (helix to ring)

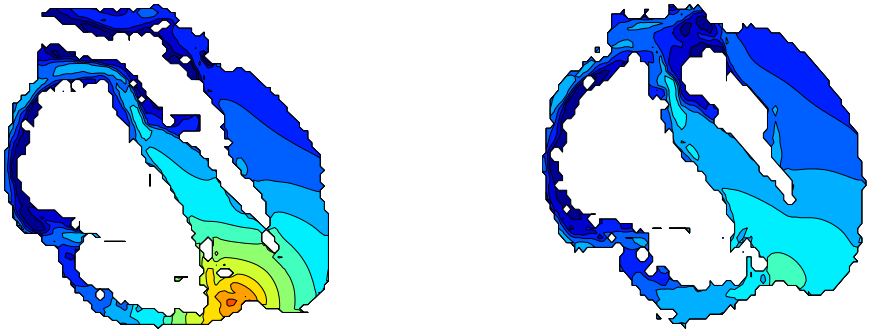

Integrated bipolar configuration (helix to coil)

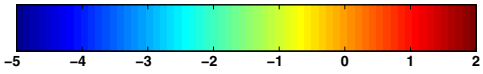

Fig. 2. Sensitivity distributions of bipolar intracardiac configurations at two cross-sections of the heart (arbitrary units, logarithmic scale).

	Discrimination power (dB)	
	DI_{AV}	DI_{MV}
Unipolar *A*	-33	-13
Unipolar *B*	-15	-2
Dedicated bipolar	-61	-57
Integrated Bipolar	-48	-50

Table 3. Discrimination power against atrial and muscular artifacts.

5. Conclusions

Current ICD tachyarrhythmia detection algorithms use heart rhythm criteria to determine whether patients are suffering from a life-threatening arrhythmia. In order to extract heart rhythm, ICD currently estimate the duration of the RR interval on a beat-to-beat basis by sensing ventricular activations in EGM signals, which are continuously recorded by intracardiac leads. As a consequence, ICD overall performance depends on the ability of intracardiac leads to measure ventricular bioelectric events and reject other biolectric events of non-ventricular origin, which include myopotentials (Deshmukh & Anderson, 1998; Kowalski et al., 2008; Sandler & Kutalek, 1994; Schulte et al., 2001) and pacing stimulus artifacts (Menz et al., 1998).

It is widely acknowledged that lead design can affect EGM sensing and therefore ICD performance. On the basis that bipolar configurations are more specific to ventricular events than unipolar configurations, current ICD use bipolar leads, either dedicated or integrated, for EGM sensing, while unipolar-like leads are mainly used for cardiac defibrillation. In a previous study, the sensitivity distribution of two unipolar and two bipolar intracardiac ICD leads were investigated in a numerical model of the ventricles (Requena-Carrión et al., 2009). This study showed quantitatively that bipolar leads concentrate their measurements more than unipolar leads and therefore, provide with ventricular events at a more local level than unipolar leads, which are characterized by global measurements.

In the present study, the investigation previously developed in (Requena-Carrión et al., 2009) has been extended by including the analysis of the sensitivity distribution at the atria and near muscles. Four intracardiac leads based on a current ICD commercial system have been studied in a computational model of the human thorax. Our analysis supports the view that bipolar configurations concentrate their measurement on a local level, while unipolar configurations provide with global measurements. In addition to this, we have been able to analyze qualitatively the sensitivity distribution at the ventricular and atrial myocardium, showing that the sensitivity distribution of unipolar configurations is roughly of the same order of magnitude at the atria and at the ventricles, whereas the sensitivity distribution of bipolar configurations drops several orders of magnitude from the ventricles to the atria. In order to analyze quantitatively the sensitivity to non-ventricular bioelectric sources, we have proposed a discrimination index that compares the accumulated sensitivity at the ventricles with the accumulated sensitivity at other non-ventricular bioelectric sources. Our results reveal that bipolar configurations are more specific to ventricular sources than unipolar configurations and hence, less vulnerable to bioelectric artifacts.

The notion of lead sensitivity distribution can provide with a useful insight into the nature of bioelectric signals. In combination with numerical methods, the sensitivity distribution can help to analyze the performance of current leads and can assist in the design of future leads.

6. Acknowledgments

The authors would like to thank Dr. -Ing. Gunnar Seeman of Karlsruhe Institute of Technology for kindly providing with the detailed numerical model of the human thorax that was used in this study.

7. References

Arzbaecher, R. C., Jenkins, J. M., Collins, S. & Berbari, E. (1979). Atrial electrical activity: The view from the esophagus, *IEEE/EMBS Frontiers of Engineering in Health Care*, pp. 314–318.

Asbach, S., Weiss, I., Wenzel, B., Bode, C. & Sehender, M. (2006). Intrathoracic far-field electrocardiogram allows continuous monitoring of ischemia after total coronary occlusion, *Pacing and Clinical Electrophysiology* 29(12): 1334–1340.

Belott, P. H. & Reynolds, D. W. (2007). Permanent pacemaker and implantable cardioverter-defibrillator implantation, *in* Ellenbogen, K. A., Kay, G. N., Lau, C. P. & Wilkoff, B. L. (eds), *Clinical cardiac pacing, defibrillation, and resynchronization therapy*, Saunders/Elsevier, Philadephia, pp. 561–651.

Bunch, T. J. & Day, J. D. (2008). The diagnostic evolution of the cardiac implantable electronic device: The implantable monitor of ischemia, *Journal of Cardiovascular Electrophysiology* 19(3): 282–284.

Cooklin, M., Tummala, R. V., Peters, R. W., Shorofsky, S. R. & Gold, M. R. (1999). Comparison of bipolar and integrated sensing for redetection of ventricular fibrillation, *American Heart Journal* 138(1 Pt 1): 133–136.

DeCaprio, V., Hurzeler, P. & Furman, S. (1977). A comparison of unipolar and bipolar electrograms for cardiac pacemaker sensing, *Circulation* 56(5): 750–755.

Deshmukh, P. & Anderson, K. (1998). Myopotential sensing by a dual chamber implantable cardioverter defibrillator: Two case reports, *Journal of Cardiovascular Electrophysiology* 9(7): 767–772.

Frain, B. H., Ellison, K. E., Michaud, G. F., Koo, C. H., Buxton, A. E. & Kirk, M. M. (2007). True bipolar defibrillator leads have increased sensing latency and threshold compared with the integrated bipolar configuration, *Journal of Cardiovascular Electrophysiology* 18(2): 192–195.

Gabriel, S., Lau, R. W. & Gabriel, C. (1996). The dielectric properties of biological tissues: II. Measurements in the frequency range 10 hz to 20 Ghz, *Physics in Medicine and Biology* 41: 2251–2269.

Goldberger, J. J., Horvath, G., Donovan, D., Johnson, D., Challapalli, R. & Kadish, A. H. (1998). Detection of ventricular fibrillation by transvenous defibrillating leads: integrated versus dedicated bipolar sensing, *Journal of Cardiovascular Electrophysiology* 9: 677–688.

Gradaus, R., Breithardt, G. & Bocker, D. (2003). ICD leads: design and chronic dysfunctions, *Pacing and Clinical Electrophysiology* 26(2 Pt 1): 649–657.

Jenkins, J. M. (1992). Impact of electrode placement and configuration on performance of morphological measures of intraventricular electrograms, *IEEE Computers in Cardiology*, pp. 367–370.

Kowalski, M., Ellenbogen, K. A., Wood, M. A. & Friedman, P. L. (2008). Implantable cardiac defibrillator lead failure or myopotential oversensing? An approach to the diagnosis of noise on lead electrograms, *Europace* 10(8): 914–917.

Langberg, J. J., Gibb, W. J., Auslander, D. M. & Griffin, J. C. (1988). Identification of ventricular tachycardia with use of the morphology of the endocardial electrogram, *Circulation* 77(6): 1363–1369.

Malmivuo, J. & Plonsey, R. (1995). *Bioelectromagnetism: Principles and applications of bioelectric and biomagnetic fields*, Oxford University Press, New York.

Malmivuo, J., Suihko, V. & Eskola, H. (1997). Sensitivity distributions of EEG and MEG measurements, *IEEE Transactions on Biomedical Engineering* 44: 196–208.

Medtronic (2008). *Secura VR D224VRC*.

Medtronic (2010). *Sprint Quattro Secure 6947*.

Menz, V., Schwartzman, D., Drachman, D., Michele, J. J. & Dillon, S. M. (1998). Recording of pacing stimulus artifacts by endovascular defibrillation lead systems: Comparison of true and integrated bipolar circuits, *Journal of Interventional Cardiac Electrophysiology* 2: 269–272.

Nash, A., Fröhlig, G., Taborsky, M., Stammwitz, E., Maru, F., Bouwens, L. & Çeliker, C. (2005). Rejection of atrial sensing artifacts by a pacing lead with short tip-to-ring spacing, *Europace* 7(1): 67–72.

Natale, A., Sra, J., Axtell, K., Akhtar, M., Newby, K., Kent, V., Geiger, M. J., Brandon, M. J., Kearney, M. M. & Pacifico, A. (1996). Undetected ventricular fibrillation in transvenous implantable cardioverter-defibrillators. Prospective comparison of different lead system-device combinations, *Circulation* 93(1): 91–98.

Parsonnet, V., Myers, G. H. & Kresh, Y. M. (1980). Characteristics of intracardiac electrograms II: Atrial endocardial electrograms, *Pacing and Clinical Electrophysiology* 3(4): 406–417.

Requena-Carrión, J., Väisänen, J., Alonso-Atienza, F., García-Alberola, A., Ramos-López, F. & Rojo-Álvarez, J. L. (2009). Sensitivity and spatial resolution of transvenous leads in implantable cardioverter defibrillator, *IEEE Transactions on Biomedical Engineering* 56(12): 2773 –2781.

Requena-Carrión, J., Väisänen, J., Rojo-Álvarez, J. L., Hyttinen, J., Alonso-Atienza, F. & Malmivuo, J. (2007). Numerical analysis of the resolution of surface electrocardiographic lead systems, *FIMH*, pp. 310–319.

Rush, S. & Driscoll, D. A. (1969). EEG electrode sensitivity–an application of reciprocity, *IEEE Transactions on Biomedical Engineering* 16(1): 15–22.

Sachse, F. B., Werner, C. D., Meyer-Waarden, K. & Dössel, O. (1998). Applications of the visible man dataset in electrocardiology: Calculation and visualization of body surface potential maps of a complete heart cycle, *Second Users Conference of the National Library of Medicine's Visible Human Project*, pp. 47–48.

Sandler, M. J. & Kutalek, S. P. (1994). Inappropriate discharge by an implantable cardioverter defibrillator: Recognition of myopotential sensing using telemetered intracardiac electrograms, *Pacing and Clinical Electrophysiology* 17(4): 665–671.

Schulte, B., Sperzel, J., Carlsson, J., Dürsch, M., Erdogan, A., Pitschner, H. F. & Neuzner, J. (2001). Inappropriate arrhythmia detection in implantable defibrillator therapy

due to oversensing of diaphragmatic myopotentials, *Journal of Interventional Cardiac Electrophysiology* 5: 487–493.

Swerdlow, C. D., Gillberg, J. M. & Olson, W. H. (2007). Sensing and detection, *in* Ellenbogen, K. A., Kay, G. N., Lau, C. P. & Wilkoff, B. L. (eds), *Clinical cardiac pacing, defibrillation, and resynchronization therapy*, Saunders/Elsevier, pp. 75–160.

Takano, N. (2002). Reduction of ECG leads and equivalent sources using orthogonalization and clustering techniques, *Doctoral Thesis 302*, Ragnar Granit Institute, Tampere University of Technology.

Väisänen, J. & Hyttinen, J. (2009). Region of interest sensitivity ratio in analyzing sensitivity distributions of electrocardiographic measurements, *Annals of Biomedical Engineering* 37: 692–701.

Väisänen, J., Väisänen, O., Malmivuo, J. & Hyttinen, J. (2008). New method for analysing sensitivity distributions of electroencephalography measurements, *Medical & Biological Engineering & Computing* 46: 101–8.

Williams, J. L., Mendenhall, G. S. & Saba, S. (2008). Effect of ischemia on implantable defibrillator intracardiac shock electrograms, *Journal of Cardiovascular Electrophysiology* 19(3): 275–281.

Zaitsev, A. V., Berenfeld, O., Mironov, S. F., Jalife, J. & Pertsov, A. M. (2000). Distribution of excitation frequencies on the epicardial and endocardial surfaces of fibrillating ventricular wall of the sheep heart, *Circulation Research* 86: 408–417.

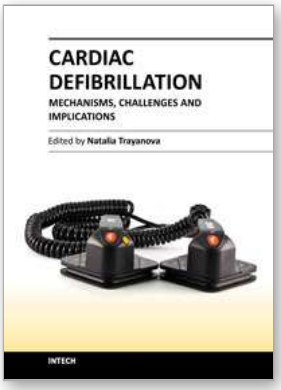

Cardiac Defibrillation - Mechanisms, Challenges and Implications

Edited by Prof. Natalia Trayanova

ISBN 978-953-307-666-9
Hard cover, 248 pages
Publisher InTech
Published online 26, September, 2011
Published in print edition September, 2011

The only known effective therapy for lethal disturbances in cardiac rhythm is deï¬brillation, the delivery of a strong electric shock to the heart. This technique constitutes the most important means for prevention of sudden cardiac death. The efficacy of defibrillation has led to an exponential growth in the number of patients receiving implantable devices. The objective of this book is to present contemporary views on the basic mechanisms by which the heart responds to an electric shock, as well as on the challenges and implications of clinical defibrillation. Basic science chapters elucidate questions such as lead configurations and the reasons by which a defibrillation shock fails. Chapters devoted to the challenges in the clinical procedure of defibrillation address issues related to inappropriate and unnecessary shocks, complications associated with the implantation of cardioverter/defibrillator devices, and the application of the therapy in pediatric patients and young adults. The book also examines the implications of defibrillation therapy, such as patient risk stratification, cardiac rehabilitation, and remote monitoring of patient with implantable devices.

INTECH
open science | open minds

InTech Europe
University Campus STeP Ri
Slavka Krautzeka 83/A
51000 Rijeka, Croatia
Phone: +385 (51) 770 447
Fax: +385 (51) 686 166
www.intechopen.com

InTech China
Unit 405, Office Block, Hotel Equatorial Shanghai
No.65, Yan An Road (West), Shanghai, 200040, China
中国上海市延安西路65号上海国际贵都大饭店办公楼405单元
Phone: +86-21-62489820
Fax: +86-21-62489821